Fenton and Photo-Fenton Nanocatalysts Revisited from the Perspective of Life Cycle Assessment

Sara Feijoo [1], Jorge González-Rodríguez [1] , Lucía Fernández [1], Carlos Vázquez-Vázquez [2] , Gumersindo Feijoo [1] and María Teresa Moreira [1,*]

[1] CRETUS Institute, Department of Chemical Engineering, Universidade de Santiago de Compostela, 15782 Santiago de Compostela, Spain; sarafeijoomoreira@yahoo.es (S.F.); jorgegonzalez.rodriguez@usc.es (J.G.-R.); lucia.fernandezf@gmail.com (L.F.); gumersindo.feijoo@usc.es (G.F.)

[2] Laboratory of Magnetism and Nanotechnology, Department of Physical Chemistry, Faculty of Chemistry, Universidade de Santiago de Compostela, 15782 Santiago de Compostela, Spain; carlos.vazquez.vazquez@usc.es

* Correspondence: maite.moreira@usc.es; Tel.: +34-8818-16792

Abstract: This study provides an overview of the environmental impacts associated with the production of different magnetic nanoparticles (NPs) based on magnetite (Fe_3O_4), with a potential use as heterogeneous Fenton or photo-Fenton catalysts in wastewater treatment applications. The tendency of Fe_3O_4 NPs to form aggregates in water makes necessary their decoration with stabilizing agents, in order to increase their catalytic activity. Different stabilizing agents were considered in this study: poly(acrylic acid) (PAA), polyethylenimine (PEI) and silica (SiO_2), as well as the immobilization of the magnetite-based catalysts in a mesoporous silica matrix, SBA-15. In the case of photo-Fenton catalysts, combinations of magnetite NPs with semiconductors were evaluated, so that magnetic recovery of the nanomaterials is possible, thus allowing a safe discharge free of NPs. The results of this study suggest that magnetic nanoparticles coated with PEI or PAA were the most suitable option for their applications in heterogeneous Fenton processes, while ZnO-Fe_3O_4 NPs provided an interesting approach in photo-Fenton. This work showed the importance of identifying the relevance of nanoparticle production strategy in the environmental impacts associated with their use.

Keywords: LCA; environmental impact; Fenton; photocatalysis; visible light; SBA15; magnetite

1. Introduction

In the era of nanotechnology, there is a growing interest in the use of nanomaterials, which is largely attributed to their characteristic high specific surface and reactivity. In this regard, nanomaterials are emerging as an interesting alternative in multiple applications in substitution of bulk chemicals, from biomedical and clinical diagnosis to their use in the field of biochemical catalysis and environmental engineering. Advanced oxidation processes (AOPs) based on the use of NPs have shown great potential for the treatment of industrial wastewaters [1–5]. These processes encompass the generation of highly reactive oxygen species (ROS), such as hydroxyl radicals ($HO^{\bullet}$), superoxide radicals ($O_2^{\bullet-}$) and singlet oxygen ($^1O_2$), which are involved in the degradation of organic matter, generally leading to more biodegradable species with less environmental impact.

One of the most widely studied AOP processes is the Fenton process, which is based on the use of iron as a catalyst to improve the oxidative potential of H_2O_2. This reaction takes place at an acid pH of around 3 [6], which favors the formation of radicals. Magnetite (Fe_3O_4) is a naturally occurring mixed iron oxide constituted by Fe(II) and Fe(III). While bulk Fe_3O_4 is ferromagnetic, Fe_3O_4 NPs are superparamagnetic, which provides them with a stronger magnetic response when exposed to

a magnetic field. This feature makes Fe_3O_4 NPs of special interest in comparison with traditional iron-based catalysts, since their magnetic nature allows easy, fast and economical separation of the NPs from the reaction medium, which facilitates their reuse in subsequent catalytic cycles [7].

Fe_3O_4 NPs have also been widely applied as supports for photocatalytic agents such as zinc oxide (ZnO) or titanium dioxide (TiO_2), which show promising catalytic and photochemical properties towards the removal of persistent organic pollutants, such as pharmaceutical and personal care products (PPCPs) and dyes [8]. The immobilization of TiO_2 or ZnO NPs in Fe_3O_4 NPs provides not only easy recovery of the photocatalyst, but also a dual-nature nanocomposite as a photo-Fenton agent.

However, there is growing concern regarding possible environmental impacts associated not only with the use of nanoparticles, but also with the synthesis phase. The fact that they provide more reactivity than the original compounds has been the driving force of research aimed at assessing their potential toxicity in terms of human health and ecosystem damage. The toxicity of nanoparticles depends on multiple factors, such as size, crystalline structure, surface coatings, or the presence of co-pollutants in the media, characteristics that may facilitate their transport through cell membranes. However, the magnetic properties of the nanoparticles allow their retention in wastewater treatment processes, preventing their release into the environment [9,10]. These two objective indicators can guide the efforts needed for risk assessment. In addition, the production process can also lead to impacts on different environmental compartments, which must be identified in order to identify the critical aspects that affect all stages of the life cycle, not only the final product, but also the resources (chemical, energy, water) and the emissions directly and indirectly associated with their synthesis and stabilization.

Fe_3O_4 NPs can be prepared through different chemical approaches, such as co-precipitation, microemulsion, sol-gel, sonochemical and thermal decomposition, solvothermal, microwave-assisted, chemical vapor deposition, and laser pyrolysis [11–15]. Among these, chemical co-precipitation is probably the most common approach, and is based on the reaction of an aqueous mixture of ferrous and ferric salts in alkaline medium that renders into Fe_3O_4 NPs with a broad size distribution, ranging from 4 to 20 nm. To produce NPs with a more homogeneous size distribution, water-in-oil microemulsion can be considered, which consists of nano-sized water droplets dispersed in an oil phase, stabilized by a surfactant at the water/oil interface. These nano-cavities are typically in the range of 10 nm and provide a confinement effect that limits the particle nucleation, growth and agglomeration [16].

On the other hand, Fe_3O_4 NPs have a strong tendency to form aggregates in water due to their high surface energy and van der Waals interactions [17]. To avoid this hindrance, Fe_3O_4 NPs can be decorated with protecting agents, including organic coatings such as polymers (polyethylene glycol, polyvinylpyrrolidone, polyvinyl alcohol, polystyrene), natural products (chitosan, gelatin, starch, ethyl cellulose), surfactants (oleic acid, lauric acid), and inorganic coatings such as metal oxides, SiO_2 or carbon [18]. However, an increase in the stability of Fe_3O_4 in water involves difficulty in recovering them and, in the worst-case scenario, an additional separation stage between water treatment cycles. An alternative of growing interest is the use of mesoporous material, used as a support for active chemical agents due to its large surface area, mechanical and chemical stability.

Considering an integrated approach of the Fenton process and photocatalysis, the combination of a semiconductor such as TiO_2 or ZnO with a magnetic nanocomposite allows the effective separation of the reaction medium through the application of a magnetic field [19]. From the point of view of chemical synthesis, the process presents the complexity of integrating both routes, and the efficiency of the nanocatalyst can be affected in relation to its properties, such as surface, adsorption, reflectance, adhesion, and transport properties.

When it comes to assessing the environmental impacts of NP production and use, the Life Cycle Assessment (LCA) methodology arises as the most updated and comprehensive approach [20], based on international standards (ISO 14040/44) [21]. Available LCA studies of nanomaterials include nanomaterials such as CdTe, carbon nanofibres (CNFs) and nanotubes (CNTs), nanoclay (ONMT, organically modified montmorillonite), nanoscale Pt-group metals, nanocrystaline-Si, Ag, titanium

and titanium oxide, and magnetic NPs [22–25]. However, to date, no LCA reports have been found on NP production routes for Fenton and photo-Fenton applications.

The aim of this work is to benchmark the different nanostructured materials used as Fenton and photo-Fenton catalysts. The synthesis of Fe_3O_4 NPs used as Fenton agents will consider their steric or electrostatic stabilization, as well as their immobilization in SBA-15 mesoporous matrix. The synthesis of hybrid nanocomposites of TiO_2 or ZnO NPs supported onto Fe_3O_4 NPs will also be considered. The nanocatalysts with the most benign environmental profiles from the different groups will be selected on the basis of the environmental indicators associated with the production process as well as their catalytic capacity for oxidation of different dyes, chosen as model compounds of organic pollutants. Both analyses will provide additional information that will serve as criteria in the decision-making process to identify the most suitable AOP nanocatalyst.

2. Results

The proposal of any process under development which aims at replacing more developed alternatives must clearly demonstrate the expected benefits, not only from the point of view of technological feasibility and cost, but also of the environmental impacts associated with the process to be developed. What is the point if the global analysis shows that beyond the capability of certain NPs to degrade target chemicals with high performance, we are introducing higher environmental loads associated with the production of the nanocatalyst?

The assessment of the environmental impacts associated with the production of NPs was based on inventory data obtained on a pilot scale. In this case, it should be noted that all the data related to the production of nanoparticles correspond to real data, where the production protocol is presented in the materials and method section. Tables 1 and 2 present the Life Cycle Impact Assessment results for the different production routes of Fenton catalysts and photocatalysts. The different routes in terms of impact categories highlight that the synthesis protocols for the different NP present a great variability in the results obtained, identifying that the use of energy and chemical products during NP synthesis presents a significant and often dominant part of the environmental impacts of the total life cycle.

**Table 1.** Life Cycle Impact Assessment results for different types of Fenton catalysts.

	Fe_3O_4	Fe_3O_4-SiO_2	Fe_3O_4-SiO_2SBA15	Fe_3O_4-PEI	Fe_3O_4-PEISBA15	Fe_3O_4-PAA	Fe_3O_4-PAA SBA15
Climate change (CC), kg $CO_{2,eq}$	$5.33 \cdot 10^{-2}$	1.86	20.3	$1.49 \cdot 10^{-1}$	6.94	$7.90 \cdot 10^{-2}$	6.94
Ozone depletion (OD), kg CFC-11$_{eq}$	$8.21 \cdot 10^{-9}$	$1.59 \cdot 10^{-7}$	$2.67 \cdot 10^{-6}$	$2.05 \cdot 10^{-8}$	$8.64 \cdot 10^{-7}$	$1.29 \cdot 10^{-8}$	$8.64 \cdot 10^{-7}$
Terrestrial acidification (TA), kg $SO_{2,eq}$	$3.26 \cdot 10^{-4}$	$8.75 \cdot 10^{-3}$	$1.20 \cdot 10^{-1}$	$8.86 \cdot 10^{-4}$	$3.95 \cdot 10^{-2}$	$4.79 \cdot 10^{-4}$	$3.95 \cdot 10^{-2}$
Freshwater eutrophication (FE), kg P_{eq}	$1.37 \cdot 10^{-5}$	$4.35 \cdot 10^{-4}$	$6.30 \cdot 10^{-3}$	$4.54 \cdot 10^{-5}$	$2.14 \cdot 10^{-3}$	$2.46 \cdot 10^{-5}$	$2.14 \cdot 10^{-3}$
Marine eutrophication (ME), kg N_{eq}	$1.12 \cdot 10^{-5}$	$2.97 \cdot 10^{-4}$	$4.11 \cdot 10^{-3}$	$3.91 \cdot 10^{-5}$	$1.43 \cdot 10^{-3}$	$1.75 \cdot 10^{-5}$	$1.42 \cdot 10^{-3}$
Toxicity (TOX), kg 1,4-DCB$_{eq}$	$1.90 \cdot 10^{-2}$	$5.32 \cdot 10^{-1}$	7.32	$5.53 \cdot 10^{-2}$	2.38	$3.18 \cdot 10^{-2}$	2.38
Fossil depletion (FD), kg oil$_{eq}$	$1.67 \cdot 10^{-2}$	1.01	5.82	$3.98 \cdot 10^{-2}$	1.99	$2.34 \cdot 10^{-2}$	1.99

Table 2. Life Cycle Impact Assessment results for different photocatalysts.

	Fe_3O_4/ZnO	Fe_3O_4/TiO_2
Climate change (CC), kg $CO_{2,eq}$	1.78	6.08
Ozone depletion (OD), kg CFC-11$_{eq}$	$1.66 \cdot 10^{-7}$	$8.30 \cdot 10^{-7}$
Terrestrial acidification (TA), kg $SO_{2,eq}$	$7.99 \cdot 10^{-3}$	$3.77 \cdot 10^{-2}$
Freshwater eutrophication (FE), kg P_{eq}	$5.91 \cdot 10^{-4}$	$1.88 \cdot 10^{-3}$
Marine eutrophication (ME), kg N_{eq}	$2.91 \cdot 10^{-4}$	$1.31 \cdot 10^{-3}$
Toxicity (TOX), kg 1,4-DCB$_{eq}$	$5.25 \cdot 10^{-1}$	2.29
Fossil depletion (FD), kg oil$_{eq}$	$6.00 \cdot 10^{-1}$	1.71

When analyzing the environmental profile of NPs considered to be Fenton catalysts, two distinct groups are observed: the stabilized magnetite NPs and those with a surface coating (Group 1); and those that have been immobilized in a mesoporous matrix (Group 2). It is evident that there are notable differences between the NPs belonging to one group and those belonging to the other, so that the environmental impacts associated with mesoporous NPs are excessively high in comparison with those produced with a simpler procedure. Accordingly, the high environmental impact of the Fe_3O_4 NPs onto the SBA-15 matrix can be explained attending to the use of additional chemicals needed to produce the mesoporous silica, as well as the electricity used during the heating stages required to carry out the reaction.

When analyzing in detail the different routes, it is also evident that some of the alternatives evaluated resemble each other due to the comparable production of nanoparticles, similar use of chemicals and electricity, and minor differences in the amount of chemicals used to adjust pH, water consumption for the washing stages, and similar wastewater flows generated. These similarities are especially evident for the production of Fe_3O_4, Fe_3O_4@PEI and Fe_3O_4@PAA NPs, which present similar environmental profiles and limited impacts, clearly lower than those of silica-coated NPs with a more complex production scheme (Figure 1). Beyond the stages common to the different pathways, the main differences are related to the complexity of the downstream stages necessary for the final formulation of the different nanoparticles. On the other hand, during the production of Fe_3O_4@SiO_2 NPs, cyclohexane is used in the re-dispersion and in the reaction stages, which represents more than 25% of the impact of chemicals in the manufacturing process. From an environmental point of view, the use of PEI or PAA coated NPs would be recommended, even preferentially to the sterically stabilized ones. Although the latter have less impact, they also tend to agglomerate in a shorter period of time, so that their operational stability may be compromised.
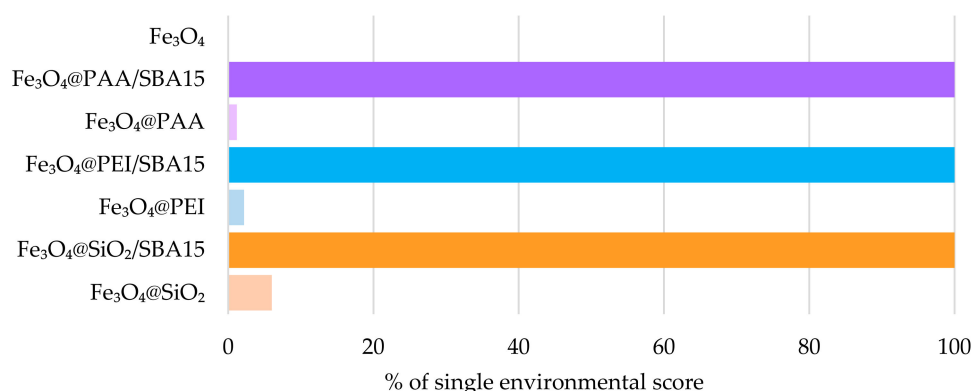

Figure 1. Benchmarking relative values of single environmental scores for the synthesis routes of magnetic NPs.

When reporting the results of nanoparticles used for photocatalysis, the environmental impact of Fe_3O_4/ZnO production show values comparable to those of silica-coated NPs, but there is a clear difference when assessing the impacts of Fe_3O_4/TiO_2 nanocomposite, which implies a substantial increase in the normalized environmental impact up to $7.1 \cdot 10^{-2}$ (Figure 2).

Beyond the environmental impacts of their production, the focus should be on considering these indicators and the oxidation potential of nanocatalysts towards a target compound. For this purpose, a selection of those nanocatalysts with promising results from each group were evaluated for the removal of Reactive Blue 19 (RB19), Congo Red (CR), Orange II (OII) and Methyl Green (MG), which were selected as models of organic pollutants.

Degradation depends on multiple factors, such as the interaction between catalysts and compounds, the stability of the catalyst, the size of the nanoparticles or the specific surface. The surface charge of the nanoparticles studied was measured: only Fe_3O_4@PEI was positively charged, with a zeta potential of 29.9 mV. The other Fenton catalysts had surface loads of −11.5, −14.0 and −14.3 mV for

Fe_3O_4, $Fe_3O_4@PAA$, and $Fe_3O_4@SiO_2$, respectively (Figure 3). The size distribution of the magnetite nanoparticles was about 10 nm, and in the case of the silica-coated catalyst, the thickness of the shell was about 5 nm. More specific data on the characterization of nanoparticles can be found in the list of references corresponding to the methodology section.
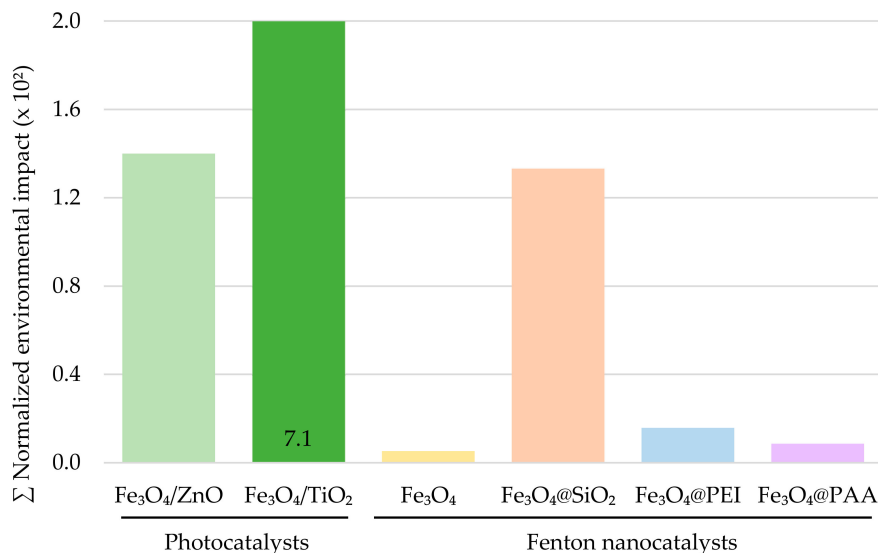
Figure 2. Environmental impacts associated with the synthesis routes of magnetic NPs.
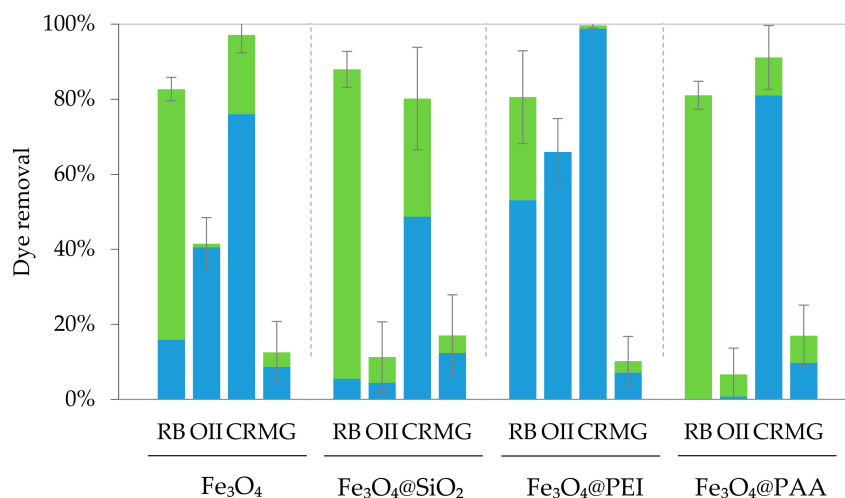
Figure 3. Percentage of dye adsorption (blue) and degradation (green) for C_0 = 10 mg L^{-1} after 3 h of Fenton (300 mg L^{-1} of catalyst, 300 mg L^{-1} of H_2O_2, pH 3).

Depending on the type of dye, the decolorization results are different: the RB19 dye is degraded more extensively than the MG dye, whose degradation is in the best-case scenario lower than 20%. Surprisingly, the performance of the Fe_3O_4/ZnO photocatalyst was superior to that of the Fenton catalysts, reaching elimination levels close to 100%. However, for the other dyes, its performance was clearly lower, with removal percentages below 50% (data not shown). As for the Fenton catalysts, the performance of the different alternatives in terms of dye removal was quite similar in all cases, but the stability of the catalysts improved with the addition of coatings. It was observed that the coating of nanoparticles with PEI substantially improved the adsorption of the target compounds due to their surface load, but the degradation values for this nanocatalyst were very low. The results also show the influence of the type of the target compound on degradation, related to the surface charge and the interaction between the dye and the nanoparticle.

The reuse of nanoparticles is interesting for wastewater treatment applications, as the costs associated with catalyst production are reduced. Selected nanoparticles include bare magnetite nanoparticles, as a basis for comparison, and other nanoparticles with different coatings. On the one hand, organic coatings with PAA and PEI provide stabilization, because the repulsive forces between these chemically bonded polymers and the nanoparticles reduce the super-paramagnetic interactions of the nanostructured magnetite. On the other hand, the coating with SiO_2 provides stability by forming a layer around the magnetic nanoparticles. In addition, the immobilization of semiconductor photocatalysts on magnetic supports allows separation by applying a magnetic field, improving recovery.

Considering the combination of technical and environmental perspectives, although the nanocomposite PAA-coated Fe_3O_4/SBA15 could be preferred among the different alternatives, the environmental impact was significantly greater for this option. Considering a balance between efficiency and impact results, a preferred option is the option of PAA-coated Fe_3O_4 as it combines catalytic potential, simplicity in production, magnetic separation of the catalyst and low environmental impact.

3. Materials and Methods

3.1. Reagents

Tetraethyl orthosilicate (TEOS, 98% *w/w*), iron(III) chloride hexahydrate ($FeCl_3 \cdot 6H_2O$, 97% w/w), zinc(II) acetate dihydrate ($Zn(CH_3COO)_2 \cdot 2H_2O$, ≥98% w/w), titanium(IV) isopropoxide ($Ti(OCH(CH_3)_2)_4$, ≥97% *w/w*), hydrochloric acid (HCl, 37% *w/w*), cyclohexane (C_6H_{12}, 99.8% *w/w*), Igepal CO-520 (polyoxyethylene (5) nonylphenylether, branched), polyacrylic acid (PAA, Mw 2000), polyethylenimine (PEI, Mw 25000), triblock copolymer Pluronic P123 (PEO20-PPO70-PEO20), 2-propanol (($CH_3)_2CHOH$, ≥99.5% *w/w*), Reactive Blue 19 (RB19, ≈50% *w/w*), Congo Red (CR, ≥85% *w/w*), Orange II (OII, ≥85% *w/w*), Methyl Green (MG, 85% *w/w*) and hydrogen peroxide (H_2O_2, 30% *w/w*) were obtained from Sigma-Aldrich (St. Louis, MI, USA). Iron(II) sulfate heptahydrate ($FeSO_4 \cdot 7H_2O$, 99% *w/w*), ortho phosphoric acid (H_3PO_4, 85% *w/w*), tetramethylammonium hydroxide (TMAOH, ≈10% *w/w*) and ammonium hydroxide (NH_4OH, 28% *w/w*) from Fluka (Buchs, ZU, Switzerland); ethanol (CH_3CH_2OH, 99.9% *w/w*) and acetone (CH_3COCH_3, ≥99% *w/w*) were purchased from Scharlau (Sentmenat, CT, Spain), and oleic acid (cis-9-octadecenoic acid, $CH_3(CH_2)_7CH=CH(CH_2)_7COOH$, extra pure) from Merck (Darmstadt, HE, Germany). Milli-Q deionized water was used in all the experiments and were purchased from Merck-Millipore (Darmstadt, HE, Germany).

3.2. Goal and Scope Definition

The purpose of this work is to evaluate the environmental performance of different types of nanoparticles as Fenton and photo-Fenton catalysts based on the use of magnetite NPs stabilized with surfactants or coatings, immobilized on mesostructured materials or combined with semiconductors. The selected nanoparticles are listed in Table 3.

Table 3. Selected nanoparticles used in different AOPs description.

AOP Type	Nanocatalyst Code	Nanocatalyst Description
Fenton process	Fe_3O_4	Magnetite NPs
	Fe_3O_4@PAA	Poly(acrylic acid) coated magnetic NPs
	Fe_3O_4@PEI	Polyethylenimine coated magnetic NPs
	Fe_3O_4@SiO_2	Silica coated magnetic NPs
	Fe_3O_4@PAA/SBA15	Poly(acrylic acid) coated magnetic NPs supported onto SBA-15
	Fe_3O_4@PEI/SBA15	Polyethylenimine coated magnetic NPs supported onto SBA-15
	Fe_3O_4@SiO_2/SBA15	Silica coated magnetic NPs supported onto SBA-15
Photocatalysis process	Fe_3O_4/TiO_2	Titanium dioxide magnetic nanocomposite
	Fe_3O_4/ZnO	Zinc oxide magnetic nanocomposite

3.3. Description of the Different Production Processes

3.3.1. Sterically Stabilized Magnetite

In a typical synthesis, $FeCl_3$ (45 mmol) and $FeSO_4$ (Fe^{3+}/Fe^{2+} molar ratio $\approx$ 1.5) are dissolved in a 100 mL of 0.01 M HCl solution. Temperature increased to 60 °C in a 250 mL round-bottom flask, using 30 mL of NH_4OH (28% *w/w*) in a subsequent step to promote the formation of black magnetite nanoparticles. The nanoparticles were washed three times with deionized water and, finally, a tetramethylammonium hydroxide (TMAOH) solution (10% *w/w*) was added to reach pH 10 to obtain sterically stabilized magnetite [25]. Both the energy consumption associated with agitation and heating (60 °C) and the consumption of deionized water for redispersion and washing were considered in the computation of inventory data. Oleic acid (OA) is a surfactant commonly used to stabilize black magnetite nanoparticles, although it can be considered as an intermediate step in the formulation of more complex NPs, such as those coated with silica. For this purpose, Fe_3O_4 NPs are exposed to an OA solution until flocculation occurs.

3.3.2. Mesostructured Silica Synthesis

The procedure for producing mesoporous ordered silica SBA-15 was based on the Colilla method [26], using a Pluronic P123 (PEO20-PPO70-PEO20) triblock copolymer, HCl/H_3PO_4 and TEOS. The product was dried and subjected to different washing cycles with organic solvents to remove the remaining block copolymer [27]. For the life cycle inventory (LCI) estimation, the energy consumption associated with agitation (24 h), heating (35–100 °C) and drying (60 °C) and the consumption of isopropyl alcohol for washing were considered.

3.3.3. Synthesis of Iron Oxide Supported in Mesostructured Silica

The addition of SBA-15 to the solvothermal preparation of Fe_3O_4 NPs allowed to obtain multi-core magnetic mesoporous nanocomposites [27]. As in previous protocols, the energy consumption associated with mechanical stirring and drying (60 °C) and the consumption of ethanol and distilled water for washing were considered.

3.3.4. Polyethylenimine (PEI)-Coated and Polyacrylic Acid (PAA)-Coated Magnetite Nanoparticles

The production process starts with the addition of PEI or PAA to Fe_3O_4 NPs, with the addition of HCl to lower the pH to 4 before the addition of tetraethyl orthosilicate (TEOS) to produce mNP [28]. For the LCI estimation, the energy consumption associated with mechanical stirring and drying (60 °C) and the consumption of ethanol and distilled water for washing were considered.

3.3.5. Silica-Coated Magnetic Nanoparticles

$Fe_3O_4@SiO_2$ core-shell nanoparticles were prepared through a water-in-cyclohexane reverse microemulsion starting from the oleic-acid-coated magnetite nanoparticles [25], using as main chemicals: polyoxyethylene(5)nonylphenyl ether (Igepal CO-520), cyclohexane, NH_4OH, TEOS and isopropanol (IPA) [29]. Beyond the consumption of chemicals and the energy consumption associated with mechanical stirring and drying (60 °C), the consumption of distilled water and cyclohexane for washing and redispersion were also included.

3.3.6. Preparation of Nanocomposites (NC) of $Fe_3O_4@PAA/SBA-15$ and $Fe_3O_4@PEI/SBA-15$

The nanocomposites were synthesized by incorporating the SBA-15 matrix in a container with an aqueous solution of HCl, $FeCl_3 \cdot 6H_2O$ and $Fe(SO_4)_2 \cdot 4H_2O$ under mechanical agitation. The temperature increased to 60 °C and NH_4OH and PAA (Mw 2000 Da) ($Fe_3O_4@PAA/SBA-15$) or PEI (Mw 25000 Da) were added to the mixture. The reaction was allowed to progress for 1 h, and the resulting precipitate was acidified to pH 4 with HCl (9%), and then magnetically separated. Finally, the NC were repeatedly

washed with distilled water and ethanol and dried at 60 °C for 12 h [28]. For the LCI estimation, the energy consumption associated with mechanical stirring and drying (60 °C) and the consumption of ethanol and distilled water for washing were considered.

3.3.7. Preparation of the Nanoparticles $Fe_3O_4@SiO_2$/SBA-15

This procedure was based on the formation of silica-coated NPs in water-in-oil microemulsion systems, but including the SBA-15 matrix to favor the anchoring of $Fe_3O_4@SiO_2$ on the external surface of the SBA-15 matrix [29]. Finally, the reaction was continued at room temperature for 16 h, under mechanical stirring and in the dark. After the reaction was completed, isopropyl alcohol (IPA) was added to precipitate the material; the supernatant was separated from the magnetic solid with the help of a magnet. The sample was further washed several times with ethanol and deionized H_2O. Finally, the sample was filtered and dried at 60 °C for 24 h. In this case, the consumption of energy for mechanical stirring comprised several production phases: stage I (15 min), stage II (20 min), stage III (16 h) and drying (60 °C).

3.3.8. Synthesis of Fe_3O_4/ZnO Nanocomposite

The synthesis of Fe_3O_4/ZnO nanocomposite was based on the preparation of polyol-mediated ZnO nanoparticles [30], using 10 mL of diethyleneglycol (DEG) mixed with 100 mL of 90 mM Zn(II) acetate, in combination with 50 mg of sterically stabilized magnetite (TMAOH) obtained in previous steps. The mixture was heated at 180 °C for 2 h under mechanical agitation, and the as-prepared hybrid nanoparticles were centrifuged at 7500 rpm for 15 min. Then, they were washed four times with ethanol and magnetically separated. Finally, the hybrid nanoparticles were redispersed into ethanol at a concentration of approximately 1.5% determined by thermogravimetric analysis by Perkin Elmer TGA 7 (Waltham, MA, USA). For the LCI estimation, the energy consumption associated with mechanical stirring, heating (180 °C) and centrifugation and the consumption of ethanol for washing and redispersion were considered.

3.3.9. Synthesis of Fe_3O_4/TiO_2 Nanocomposite

The synthesis of $Fe_3O_4@TiO_2$ was based on the hydrolysis and polycondensation of titanium alkoxide, added dropwise to a mixture of TMAOH and 2-propanol [31]. After 10 min, the reaction mixture was heated to 95 °C and reaction was continued for 24 h. The preparation of the nanocomposite required energy associated with cooling (2 °C, ice and water bath), mechanical stirring: stage I (10 min) and stage II (24 h), heating (95 °C) and centrifugation as well as ethanol for washing and redispersion.

3.4. Life Cycle Assessment Methodology and Assumptions

The LCA is a tool for evaluating the environmental impacts of products or processes, analyzing the inputs and the outputs of a defined system. The LCA methodology comprises four steps: scope definition, inventory analysis, impact assessment and interpretation of results. In the first step, the boundaries of the system and the functional unit in each case study are defined. By applying this definition and limits, it is possible to identify mass and energy balances. The next step is inventory analysis, in which information on both input and output flows is compiled and sorted. In the impact assessment stage, the inventory flows are associated with their contributions to the impact categories defined by the methodology used (e.g., CML, IMPACT2001 or ReCiPe). These categories are variable, depending to the method chosen, e.g., climate change (CC), ozone depletion (OD), freshwater eutrophication (FEU), or terrestrial acidification (TA). The values obtained can be analyzed and discussed at the stage of interpretation of results and are useful for comparing different alternatives or for evaluating the environmental impact of a process or product [20].

To improve the comparison between the results, a normalized value for impact can be calculated, as the weighted sum of the impact categories considering their relative contribution. The factors used in this step can be provided using different methodologies. This standardization makes it possible to

obtain a global parameter of the environmental impact, allowing the comparison between categories, establishing relative weights between them and improving the understanding of the data.

The LCA performed was based on a cradle-to-gate approach, from the production of the raw materials to the formulation of the NPs. The weight of NP produced per batch was selected as the functional unit (FU), so that it was easier to compare relative consumption of raw materials, water, chemicals, and energy, which were considered primary data obtained from the average values corresponding to different production batches. The experimental procedures for the synthesis of nanoparticles were used to calculate the main inputs and outputs. The Ecoinvent®database (2016) was used to collect background data.

Data uncertainty modeling is an interesting approach for identifying the possible robustness of the analysis and inventory data. Uncertainty in life cycle analysis is often related to the determination of relevant data, e.g., consumption or emissions figures. All the data related to the production of nanoparticles correspond to real data, where the production protocol is presented in the materials and method section. This is why they are representative and accurate data. Another option is to consider the uncertainty related to the secondary data. Since "true" values (especially for background data) are often unknown, it is virtually impossible to completely avoid uncertainty in LCA. Stochastic modeling, which can be performed by Monte Carlo simulation, is a promising technique for addressing data inaccuracy in LCI, but it is beyond the scope of this work.

The characterization factors reported by the ReCiPe methodology for Life Cycle Impact Assessment (LCIA) were used [32], a method based on the ISO standards for LCA [33]. The impact potentials evaluated were: climate change (CC), ozone depletion (OD), terrestrial acidification (TA), freshwater eutrophication (FEU), marine eutrophication (MEU), human toxicity (HT), photochemical oxidants formation (POF), terrestrial ecotoxicity (TE), freshwater ecotoxicity (FE), marine ecotoxicity (ME), water depletion (WD), and fossil depletion (FD). The software SimaPro 8.2.0 (PRé Sustainability, Amersfoort, UT, The Netherlands, 2016) was used for the computational implementation of the inventories.

3.5. Removal of Target Dyes by Fenton and Photo-Fenton Nanocatalysts

Degradation tests were carried out on nanocatalysts with better environmental profiles more environmentally friendly for the degradation of Reactive Blue 19 (RB19), Congo Red (CR), Orange II (OII) and Methyl Green (MG), selected as models of organic pollutants. The oxidative conditions were as follows: 10 mg L^{-1} dye, 300 mg L^{-1} catalyst, 300 mg L^{-1} H$_2$O$_2$, in 10 mL H$_2$O at pH 3 in Fenton applications, or pH 7 in UVA-assisted photocatalysis using a PenRay®Lamp (Analytik Jena, Jena, TH, Germany). For the calibration of the spectrophotometer PowerWave XS2 (BioTek, Winnoski, VT, USA), standard solutions of dyes with different concentrations were prepared and absorbance at the optimal wavelength was correlated with concentration for each dye.

4. Conclusions

An LCA perspective for the production of magnetite-based NPs applied in catalytic oxidation processes for wastewater treatment highlights the importance of assessing the environmental profile associated with the different production routes. Energy and chemical consumption are the dominant impacts during NP synthesis. As for Fenton, the simplest option of sterically stabilized magnetite shows fewer impacts, but the use of the nanocomposites, despite their higher contributions to environmental categories, arises as a much more advisable alternative due to the combination of transformation potential and reactivity. Similarly, in photocatalysis, when it comes to selecting the best option, the nanocomposite has better performance and even faster reaction kinetics compared to Fenton. Specifically, Fe$_3$O$_4$@PAA/SBA15 and Fe$_3$O$_4$/ZnO magnetic nanocomposites are the most reliable options over the other catalytic supports for Fenton and photo-Fenton processes.

Conflicts of Interest: The authors declare no conflict of interest.

References

1. Esplugas, S.; Giménez, J.; Contreras, S.; Pascual, E.; Rodríguez, M. Comparison of different advanced oxidation processes for phenol degradation. *Water Res.* **2002**, *36*, 1034–1042. [CrossRef]
2. Bautista, P.; Mohedano, A.F.; Casas, J.A.; Zazo, J.A.; Rodriguez, J.J. An overview of the application of Fenton oxidation to industrial wastewaters treatment. *J. Chem. Technol. Biotechnol.* **2008**, *83*, 1323–1338. [CrossRef]
3. Sayed, M.; Khan, J.A.; Shah, L.A.; Shah, N.S.; Khan, H.M.; Rehman, F.; Khan, A.R.; Khan, A.M. Degradation of quinolone antibiotic, norfloxacin, in aqueous solution using gamma-ray irradiation. *Environ. Sci. Pollut. Res.* **2016**, *23*, 13155–13168. [CrossRef] [PubMed]
4. Yu, K.; Gu, C.; Boyd, S.A.; Liu, C.; Sun, C.; Teppen, B.J.; Li, H. Rapid and Extensive Debromination of Decabromodiphenyl Ether by Smectite Clay-Templated Subnanoscale Zero-Valent Iron. *Environ. Sci. Technol.* **2012**, *46*, 8969–8975. [CrossRef]
5. Peller, J.R.; Mezyk, S.P.; McKay, G.; Watson, E. Hydroxyl Radical Probes for the Comparison of Secondary Treated Wastewaters. *Water Reclam. Sustain.* **2014**, 247–263. [CrossRef]
6. Babuponnusami, A.; Muthukumar, K. A review on Fenton and improvements to the Fenton process for wastewater treatment. *J. Environ. Chem. Eng.* **2014**, *2*, 557–572. [CrossRef]
7. Wang, N.; Zheng, T.; Zhang, G.; Wang, P. A review on Fenton-like processes for organic wastewater treatment. *J. Environ. Chem. Eng.* **2016**, *4*, 762–787. [CrossRef]
8. Lee, K.M.; Lai, C.W.; Ngai, K.S.; Juan, J.C. Recent developments of zinc oxide based photocatalyst in water treatment technology: A review. *Water Res.* **2016**, *88*, 428–448. [CrossRef] [PubMed]
9. Turan, N.B.; Erkan, H.S.; Engin, G.O.; Bilgili, M.S. Nanoparticles in the aquatic environment: Usage, properties, transformation and toxicity—A review. *Process Saf. Environ. Prot.* **2019**, *130*, 238–249. [CrossRef]
10. Brar, S.K.; Verma, M.; Tyagi, R.D.; Surampalli, R.Y. Engineered nanoparticles in wastewater and wastewater sludge—Evidence and impacts. *Waste Manag.* **2010**, *30*, 504–520. [CrossRef]
11. Maity, D.; Choo, S.-G.; Yi, J.; Ding, J.; Xue, J.M. Synthesis of magnetite nanoparticles via a solvent-free thermal decomposition route. *J. Magn. Magn. Mater.* **2009**, *321*, 1256–1259. [CrossRef]
12. Hou, Y.; Yu, J.; Gao, S. Solvothermal reduction synthesis and characterization of superparamagnetic magnetite nanoparticles. *J. Mater. Chem.* **2003**, *13*, 1983–1987. [CrossRef]
13. Kostyukhin, E.M.; Kustov, L.M. Microwave-assisted synthesis of magnetite nanoparticles possessing superior magnetic properties. *Mendeleev Commun.* **2018**, *28*, 559–561. [CrossRef]
14. Monárrez-Cordero, B.E.; Amézaga-Madrid, P.; Hernández-Salcedo, P.G.; Antúnez-Flores, W.; Leyva-Porras, C.; Miki-Yoshida, M. Theoretical and experimental analysis of the aerosol assisted CVD synthesis of magnetite hollow nanoparticles. *J. Alloys Compd.* **2014**, *615*, S328–S334. [CrossRef]
15. Morjan, I.; Alexandrescu, R.; Scarisoreanu, M.; Fleaca, C.; Dumitrache, F.; Soare, I.; Popovici, E.; Gavrila, L.; Vasile, E.; Ciupina, V.; et al. Controlled manufacturing of nanoparticles by the laser pyrolysis: Application to cementite iron carbide. *Appl. Surf. Sci.* **2009**, *255*, 9638–9642. [CrossRef]
16. Akbarzadeh, A.; Samiei, M.; Davaran, S. Magnetic nanoparticles: Preparation, physical properties, and applications in biomedicine. *Nanoscale Res. Lett.* **2012**, *7*, 144. [CrossRef]
17. Parsai, T.; Kumar, A. Understanding effect of solution chemistry on heteroaggregation of zinc oxide and copper oxide nanoparticles. *Chemosphere* **2019**, *235*, 457–469. [CrossRef]
18. Xu, J.-K.; Zhang, F.-F.; Sun, J.-J.; Sheng, J.; Wang, F.; Sun, M. Bio and Nanomaterials Based on Fe3O4. *Molecules* **2014**, *19*, 21506–21528. [CrossRef]
19. Fernández, L.; Gamallo, M.; González-Gómez, M.A.; Vázquez-Vázquez, C.; Rivas, J.; Pintado, M.; Moreira, M.T. Insight into antibiotics removal: Exploring the photocatalytic performance of a Fe3O4/ZnO nanocomposite in a novel magnetic sequential batch reactor. *J. Environ. Manag.* **2019**, *237*, 595–608. [CrossRef]
20. Curran, M.A. Life Cycle Assessment: A review of the methodology and its application to sustainability. *Curr. Opin. Chem. Eng.* **2013**, *2*, 273–277. [CrossRef]

21. International Organization for Standardization. *ISO 14040-Environmental Management—Life Cycle Assessment—Principles and Framework*; International Organization for Standardization: Geneva, Switzerland, 2006.

22. Hischier, R.; Walser, T. Life cycle assessment of engineered nanomaterials: State of the art and strategies to overcome existing gaps. *Sci. Total Environ.* **2012**, *425*, 271–282. [CrossRef] [PubMed]

23. Gavankar, S.; Suh, S.; Keller, A.F. Life cycle assessment at nanoscale: Review and recommendations. *Int. J. Life Cycle Assess.* **2012**, *17*, 295–303. [CrossRef]

24. Upadhyayula, V.K.K.; Meyer, D.E.; Curran, M.A.; Gonzalez, M.A. Life cycle assessment as a tool to enhance the environmental performance of carbon nanotube products: A review. *J. Clean. Prod.* **2012**, *26*, 37–47. [CrossRef]

25. Feijoo, S.; González-García, S.; Moldes-Diz, Y.; Vazquez-Vazquez, C.; Feijoo, G.; Moreira, M.T. Comparative life cycle assessment of different synthesis routes of magnetic nanoparticles. *J. Clean. Prod.* **2017**, *143*, 528–538. [CrossRef]

26. Colilla, M.; Balas, F.; Manzano, M.; Vallet-Regí, M. Novel method to enlarge the surface area of SBA-15. *Chem. Mater.* **2007**, *19*, 3099–3101. [CrossRef]

27. Wang, H.; Chen, Q.W.; Yu, Y.F.; Cheng, K.; Sun, Y.B. Size-and solvent-dependent magnetically responsive optical diffraction of carbon-encapsulated superparamagnetic colloidal photonic crystals. *J. Phys. Chem. C* **2011**, *115*, 11427–11434. [CrossRef]

28. Osorio, Z.V.; Pineiro, Y.; Vazquez, C.; Abreu, C.R.; Perez, M.A.A.; Quintela, M.A.L.; Rivas, J. Magnetic nanocomposites based on mesoporous silica for biomedical applications. *Int. J. Nanotechnol.* **2016**, *13*, 648. [CrossRef]

29. Vargas-Osorio, Z.; González-Gómez, M.A.; Piñeiro, Y.; Vázquez-Vázquez, C.; Rodríguez-Abreu, C.; López-Quintela, M.A.; Rivas, J. Novel synthetic routes of large-pore magnetic mesoporous nanocomposites (SBA-15/Fe3O4) as potential multifunctional theranostic nanodevices. *J. Mater. Chem. B* **2017**, *5*, 9395–9404. [CrossRef]

30. Feldmann, C.; Jungk, H.-O. Polyol-Mediated Preparation of Nanoscale Oxide Particles. *Angew. Chem. Int. Ed.* **2001**, *40*, 359–362. [CrossRef]

31. Chemseddine, A.; Moritz, T. Nanostructuring Titania: Control over Nanocrystal Structure, Size, Shape, and Organization. *Eur. J. Inorg. Chem.* **1999**, *1999*, 235–245. [CrossRef]

32. Goedkoop, M.; Heijungs, R.; Huijbregts, M.; Schryver, A.d.; Strujis, J.; van Zelm, R. *A Life Cycle Impact Assessment Method Which Comprises Harmonised Category Indicators at the Midpoint and the Endpoint Level*; Centrum Milieukunde: Leiden, The Netherlands, 2013.

33. ISO. *ISO 14044*; ISO: Geneva, Switzerland, 2006; ISBN 5935522004.